Information system for direction finding of signal sources in the ultra-long range*

Mykhaylo Palamar[1,†], Oleksandr Liashchuk[2,†], Mykhaylo Strembitskyi[1,*,†], Andrii Chaikovskyi[1,†] and Andrii Kondratiuk[1,†]

[1] *Ternopil Ivan Puluj National Technical University, Ruska str., 56, Ternopil, 46001, Ukraine*
[2] *Main Special Monitoring Center, Kosmichna str., 1, Gorodok, Zhytomyr reg., 12265, Ukraine*

Abstract
A method is proposed for recording and processing electromagnetic signals generated by nuclear explosions, lightning discharges, oblique passive ionospheric sounding and space-weather monitoring within the very-low-frequency (VLF) band. The architecture of a modernised radiotechnical monitoring station for the VLF band is developed. Parallel analogue-to-digital conversion of measuring channels and a GPS-disciplined oscillator are employed to synchronise geographically separated stations. Specialised software is created to store and visualise the direction and location of electromagnetic signal sources.

Keywords
Very-low-frequency band, radiotechnical monitoring, analogue-to-digital converter, direction finding, filter–amplifier, field-programmable gate array (FPGA)

1. Introduction

Observation of the electromagnetic field in the very low frequency range (0.3 – 90 kHz) is used to monitor the lower ionosphere, whose state governs the propagation conditions of natural electromagnetic disturbances. Variations in the conductivity profile of the lower ionosphere influence the amplitude and phase velocity of very-low-frequency (VLF) transmitters and can thus be used to assess ionospheric conditions. Because wave-guide propagation in the Earth–ionosphere cavity is extremely sensitive to small electron-density variations, amplitude and phase changes of VLF signals serve as highly responsive indicators of anomalous ionisation. Continuous ionospheric monitoring has numerous applications, including forecasting terrestrial and space-communication conditions and satellite-navigation quality; anomalous ionisation may even precede earthquakes. [1,2]. For investigating the physical processes of low-frequency signal propagation in the Earth–ionosphere waveguide and for locating lightning discharges from a single station, it is sufficient to record only one vertical electric and two horizontal magnetic components [3].

To carry out observations of the electromagnetic field in the low-frequency band, a three-component data-acquisition system is used: electromagnetic radiation is simultaneously recorded by two magnetic loop antennas oriented north–south and west–east, and by an omnidirectional monopole antenna [4]. To increase measurement sensitivity, a fourth channel — a volumetric vertical vibrator antenna—is added [5].

Several radiotechnical-monitoring stations at the Main Special Monitoring Center had outdated electronic equipment. Specifically, the dynamic range amounted to only 80 dB, and pulse registration was performed on paper media [6]. The purpose of this work is to develop a

* *CITI'2025: 3rd International Workshop on Computer Information Technologies in Industry 4.0, June 11–12, 2025, Ternopil, Ukraine*
[1*] Corresponding author.
[†] These authors contributed equally.
palamar.m.i@gmail.com (M. Palamar); alex_liashchuk@ukr.net (O. Liashchuk); m.strembitskyy@gmail.com (M. Strembitskyi); chaikovskyi@gmail.com (A. Chaikovskyi); x.alantoo@gmail.com (A. Kondratiuk)
0000-0002-8255-8491 (M. Palamar); 0000-0002-8690-1808 (O. Liashchuk); 0000-0002-5713-1672 (M. Strembitskyi); 0000-0002-0684-2052 (A. Chaikovskyi); 0009-0004-6544-6676 (A. Kondratiuk)

modernised system for registering and analysing ultra-long-wave electromagnetic radiation with increased sensitivity and digital recording of measurements. [7, 8].

2. Mathematical representation

During numerical modelling, the following expressions were used for the vertical electric and tangential magnetic-field components created in the spherical Earth–ionosphere surface by a vertical point-dipole source [3]:

$$E_r = i\frac{M(\omega)v(v+1)P_v[\cos(\pi-\theta)]}{4a^2 h\varepsilon\omega\sin(\pi v)}, \quad (1)$$

$$H_\varphi = \frac{-M(\omega)P_v^1[\cos(\pi-\theta)]}{4ahh\varepsilon\omega\sin(\pi v)}. \quad (2)$$

The indicated field components are measured in V·s/m and A·s/m; they are presented in the spherical coordinate system { } r, , θ ϕ with its origin at the centre of the Earth. We use the following notation:
a=6375 m - is the Earth's radius,
M(ω) – is the instantaneous moment of the source in A·s·m, the angular distance between the source and observer in radians, ω is the angular frequency in s^{-1},
ε =8.854·10^{-12} dielectric constant of vacuum F/m,
h = 6·10^4 m – is the effective height of the ionosphere, i =$\sqrt{-1}$, i ν ω – is the dimensionless low-frequency propagation constant.

We use the following heuristic frequency dependence of the propagation constant based on experimental data:

$$v(f) = \frac{f-2}{6} - \frac{f}{100} \quad (3)$$

We employ the following zonal-harmonic expansions:

$$P_v[\cos(\pi-\theta)] = \frac{-\sin(\pi v)}{\pi}\sum_{n=0}^{\infty}\frac{(2n+1)P_n cos\theta}{n(n+1)-v(v+1)} \quad (4)$$

$$P_v^1[\cos(\pi-\theta)] = \frac{-\sin(\pi v)v(v+1)}{\pi sin\theta}\sum_{n=1}^{\infty}\frac{(2n+1)P_n cos\theta}{[n(n+1)-v(v-1)][n(n+1)-(v+1)(v+2)]} \quad (5)$$

where Pn(cosθ) — is a Lagrange polynomial calculated by the recursion relations

$$P_0=1, P_1=cos\theta, P_{n+1}=P_n\frac{2n+1}{n+1}cos\theta - P_{n-1}\frac{n}{n+1} \quad (6)$$

As a result, we obtain the following computational formulas for the field components:

$$E_r = \frac{-M(\omega)v(v+1)}{4a^2 h\varepsilon\omega}\sum_{n}^{\square}\frac{P_n cos\theta}{n(n+1)-v(v+1)} \quad (7)$$

$$H_{\varphi}=M(\omega)\frac{v(v+1)}{4\pi a h}\frac{1}{\sin\theta}\sum_{n=1}^{\infty}\frac{(2n+1)P_n\cos\theta}{[n(n+1)-v(v-1)][n(n+1)-(v+1)(v+2)]} \quad (8)$$

We apply a method for measuring the group velocity of an pulse to determine sources of discrete atmospheric radiation. The stability and accuracy of numerical solutions for such systems can be further analyzed using methods from differential equations with delays, as demonstrated in biosensor and neural network modeling [9-13]. These approaches ensure robust parameter estimation and error minimization, which are critical for reliable direction-finding calculations. To calculate the angle of arrival of a wave we use the following relationships:

$$P_X=\frac{-1}{2}\int_{\omega_{MIN}}^{\omega_{MAX}}\Re\{E_r,H_Y^{\text{¿}}\},\ P_Y=\frac{1}{2}\int_{\omega_{MIN}}^{\omega_{MAX}}\Re\{E_r,H_X^{\text{¿}}\},\ A=\tan^{-1}\left(\frac{P_Y}{P_X}\right) \quad (6)$$

where PX and PY – averaged components of the ultrasonic pulse propagation velocity, E_r, H_X, H_Y – are the vertical electric and orthogonal horizontal magnetic-field components respectively, Re{Z} denotes the real part of a complex quantity Z, the asterisk denotes complex conjugation, A – is the power-flux azimuth in the observer’s coordinate system, and ω_{MIN} ω_{MAX} are the lower and upper frequency limits of the receiver respectively.

Calculation of the median components of the ultrasonic pulse propagation velocity result for a model of a distributed signal center in the exact direction toward the center from the observer. When two distributed centres are applied in the source model, the resulting bearing of the source falls between them, indicating an “effective centroid”. The “weight” of an individual centre depends on its distance, source density and the amplitudes of its instantaneous moments. When the model consists of several sources located at different distances from the observer, the frequency dependence manifests itself in the angle of arrival of the wave. This is explained by the fact that the contribution of the amplitude of a particular source to the power flux depends on its distance from the observer. In this case, the daily variations in the source bearing depend on the ratio of the maximum to the minimum of the individual centers, as well as on the position of the observatory on the globe.

3. Development of the Detection System

Figure 1 shows the schematic of the reception-and-analysis apparatus used in measurements with built-in pre-amplifiers [14].

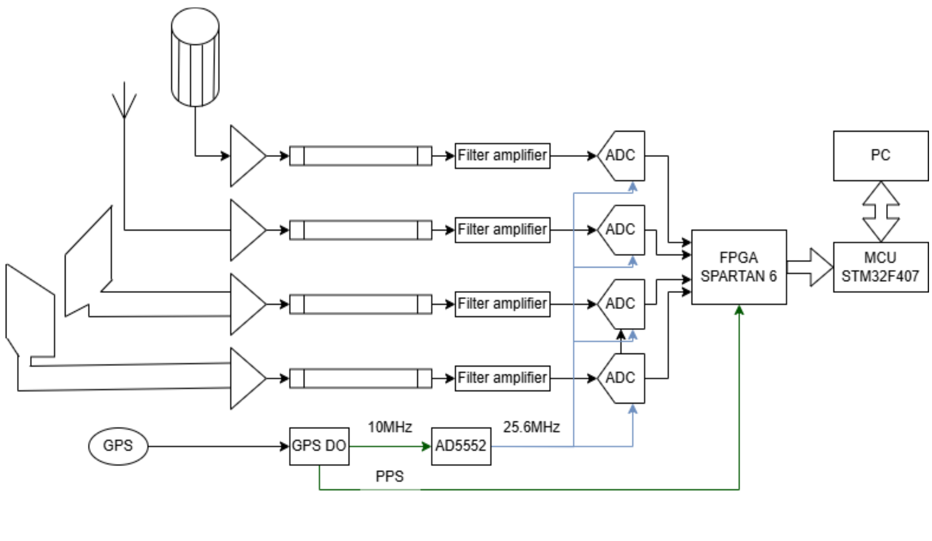

Figure 1: Structural diagram of the detection system.

The loop antenna (A2M) is oriented in the south–north and east–west directions in the geographic coordinate system. The omnidirectional monopole antenna (A1) is used to obtain direction. Antenna design optimization, such as dual-polarization Yagi arrays [15], could further enhance directional sensitivity in future iterations of this system. To increase measurement sensitivity, an antenna with a volumetric vertical vibrator ("Dunay") is used.

The data-acquisition system implements four parallel channels of analogue-to-digital conversion, which eliminates timing differences between channels that are inevitable for ADCs using channel multiplexing. The system allows the measurement of analogue signals from antennas in a frequency band up to 100 kHz with a dynamic range of 144 dB (a 24-bit sigma–delta ADC AD7768 by Analog Devices with a sampling rate of 200 kS·s⁻¹ is used). To achieve the wide dynamic range, complete galvanic isolation of the analogue and digital parts is applied. This suppresses common-mode interference even when antennas are located several kilometres from the ADC and eliminates the influence of "noisy" digital circuits on highly sensitive geophysical converters. Rigid referencing to Universal Time simplifies the joint processing of signals obtained at geographically separated stations. The time reference is established using a Trimble Thunderbolt GPS disciplined oscillator (GPSDO). Time synchronization is paramount for multi-station signal correlation. Recent advances in ROC analysis for regression models [16] highlight the importance of precision in timestamping for predictive accuracy, which aligns with our system. The GPSDO synchronises the frequency of its own 10 MHz quartz oscillator to the GPS signal with an RMS error of ±15 ns. The ADC clock frequency (25.6 MHz) is formed from the 10 MHz signal using a programmable PLL AD9552. The start of analogue-signal capture is in turn synchronised with the GPSDO one-pulse-per-second signal. The total time-stamp error of the ADC counts does not exceed 1 μs. The digitised data are transferred from the ADC to an FPGA (Spartan-6) and an STM32F407 microcontroller for time-stamp tagging. The resulting stream is sent via a 100Base-T Ethernet interface to a personal computer for recording and analysis. Similar FPGA-based architectures typically applied in telecommunication networks for radio signal detection [17], underscoring their versatility in real-time signal processing.

4. Experimental results and discussion

Figure 2 shows the main window of the data-registration program. The program allows real-time observation of the oscilloscope trace and spectrogram of the signal.

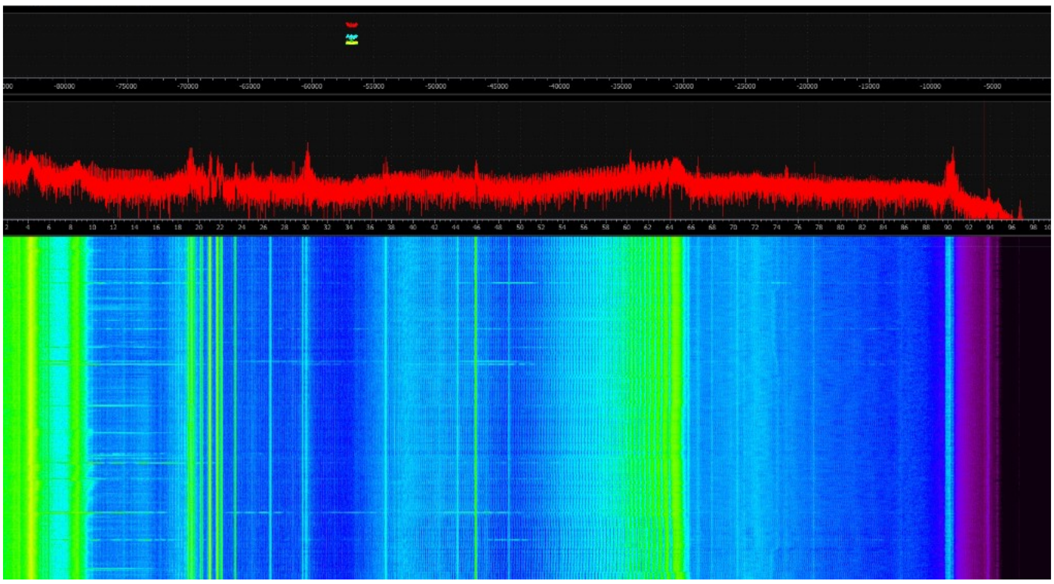

Figure 2: Graphical representation of the results of determining the object contours by maximum levels.

The recorded “raw” signal waveforms are stored in four-channel WAV files for several days. At the same time, the amplitudes of several carriers specified by the user are measured and registered. The recorded amplitude-variation profiles of reference transmitters can be used to analyse the condition of the ionosphere along the propagation path of electromagnetic radiation from the source to the receiver.

In addition, by the ratio of amplitudes and phases of the signals received by the loop and monopole antennas, the bearing of the signal source can be determined. Thus, electromagnetic atmospheric discharges of natural and anthropogenic origin can be registered. By registering a electromagnetic pulse with the aid of two or three geographically separated stations, the coordinates of the signal source can be determined. Such a system can be used for monitoring thunder-storm activity or above-ground and underground nuclear explosions.

Specialised software included in the complex is implemented as a software-mathematical algorithm for processing the obtained data. Data processing consists of the automatic detection and identification of useful pulse signals (from nuclear explosions, sferics, whistlers, etc.), estimation of the direction to the signal source, and estimation of the main signal parameters. For the ionospheric-monitoring subsystem, automatic and interactive detection of manifestations of solar flares in the ionosphere is provided (Figure 3).

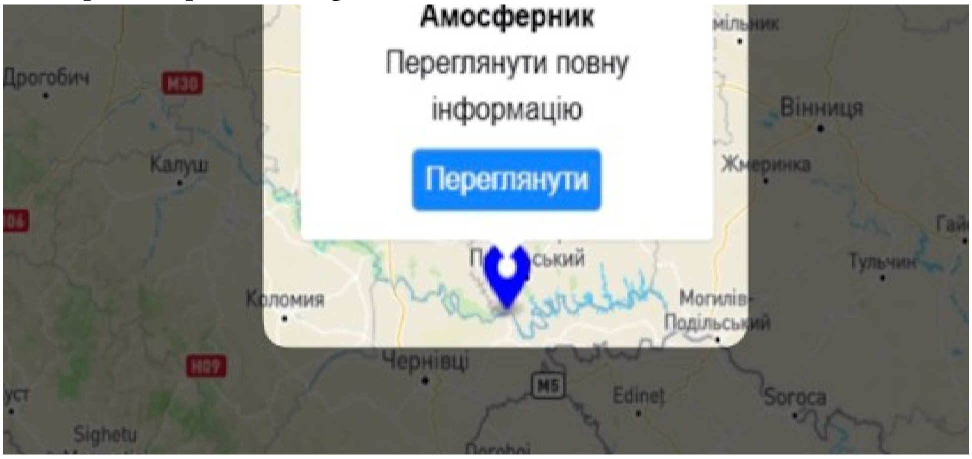

Figure 3: Graphical display of registered signals on the map.

Direction finding is performed by the discriminator method. Information about the detected signals (time, amplitude, period, azimuth, type) is formed into daily text files that have a name consisting of the station abbreviation, year and day of year. The files are stored in a separate directory. Based on the results of daily registration, a daily summary should be formed concerning the number and type of signals and the main (prevailing) azimuths to the signals. For joint processing of data from several radiotechnical complexes, instantaneous transmission/reception of information about a registered event is envisaged.

For the amplitude analyser, text files are named by channel, year and day number. The information for a day from all channels is stored in one directory that bears the day number; in turn, all daily directories are stored in a general directory named by year (Figure 4).

ID	Дата	Азимут	Амплітуда	Категорія	Станція	Lon	Lat	Дата створення
13138000	02-05-2025 07:45:52.228	117.406239001992	0.00937110371887684	Амосферник	Balta	29.609036	47.941193	02-05-2025 07:45
13137999	02-05-2025 07:45:41.597	241.904946438125	0.0109007228165865	Амосферник	Balta	29.609036	47.941193	02-05-2025 07:45
13137998	02-05-2025 07:45:22.068	269.611718089308	0.0127615369856358	Амосферник	Balta	29.609036	47.941193	02-05-2025 07:45
13137997	02-05-2025 07:44:52.086	99.5766858718339	0.0108345039188862	Амосферник	Balta	29.609036	47.941193	02-05-2025 07:44

Figure 4: List of registered signals.

When configuring the amplitude analyser (field-strength monitoring), filtering and change of the sampling period are enabled. The possibility of recording the modified signal is provided.

Filtering for spectrogram display and filtering for the processing results of the analysers (a median or similar filter for smoothing outliers) is implemented.

Conclusions

On the basis of modern components and software algorithms, a modernised hardware–software complex of the K-120-R type has been created, making it possible to increase the sensitivity and expand the functional capabilities of the system for registering and processing electromagnetic signals in the extended ultra-long-wave frequency range. Specialised software has been developed for joint processing of signals from several stations to determine the coordinates of a signal source and to automatically recognise certain types of signals (sferics, whistlers, etc.). The program ensures the control of information entered by the operator for admissible values with error messages, protection of data from erroneous operator actions, protection of data from unauthorised access, organisation of interaction with the operator by means of a dialogue using menus and prompts, and keeping a log of operator actions. The specialised software makes it possible to visualise and analyse signals in time and spectral forms, to scale signals with a change in scale and with display of measurement units, provides functions for monitoring phase variations of very-low-frequency transmitters, and ensures real-time transmission of received signals to one of the stations for processing and analysis.

Further development and refinement of the specialised-software (SPZ) algorithms is planned in order to automate the recognition of signal sources, to detect and identify new types of signals, and to analyse the state of the ionosphere.

Declaration on Generative AI

The authors have not employed any Generative AI tools.

References

[1] Brinegar, C. Passive Direction Finding: Combining Amplitude and Phase Based Methods; IEEE: Dayton, FL, USA, 2000; pp. 78–84.

[2] Ma, H.; Tao, H.; Kang, H. Mixed far-field and near-field source localization using a linear electromagnetic-vector-sensor array with gain/phase uncertainties. IEEE Access 2016, 4.

[3] Musicant, A.; Almog, B.; Oxenfeld, N.; Shavit, R. Vector sensor antenna design for VHF band. IEEE Antennas Wirel. Propag. Lett. 2015, 14, 1404–1407.

[4] Yuan, X.; Wong, K.T.; Xu, Z.; Agrawal, K. Various compositions to form a triad of collocated dipoles/loops, for direction finding and polarization estimation. IEEE Sens. J. 2012, 12, 1763–1771.

[5] Lominé, J.; Morlaas, C.; Imbert, C.; Aubert, H. Dual-band vector sensor for direction of arrival estimation of incoming electromagnetic waves. IEEE Trans. Antennas Propag. 2015, 63, 3662–3671.

[6] Pohlmann, R.; Zhang, S.; Jost, T.; Dammann, A. Power-based direction-of-arrival estimation using a single multi-mode antenna. In Proceedings of the 14th Workshop on Positioning, Navigation and Communications (WPNC), Bremen, Germany, 25–26 October 2017.

[7] Anchidin, L.; Ilie, C.-A.; Bucuci, S.; Tamas, R.; Caruntu, G. A New Insight on the Distance Averaging Method: Linear Scanning Versus Matrix Scanning; IEEE: Constanta, Romania, 2018.

[8] Tamas, R.D.; Deacu, D.; Vasile, G.; Ioana, C. A method for antenna gain measurements in nonanechoic sites. Microw. Opt. Technol. Lett. 2014, 56, 1553–1557.

[9] Martsenyuk, V., Klos-Witkowska, A., & Sverstiuk, A. (2020). Stability Investigation of Biosensor Model Based on Finite Lattice Difference Equations. In Springer Proceedings in Mathematics & Statistics (pp. 297–321). Springer International Publishing. https://doi.org/10.1007/978-3-030-35502-9_13

[10] Sverstiuk A.S. Research of global attractability of solutions and stability of the immunosensor model using difference equations on the hexagonal lattice (2019) Innovative Biosystems and Bioengineering, 3 (1), pp. 17 – 26. https://doi.org/10.20535/ibb.2019.3.1.157644.
[11] Martsenyuk V., Sverstiuk A., Andrushchak I. (2019). Approach to the study of global asymptotic stability of lattice differential equations with delay for modeling of immunosensors. Journal of Automation and Information Sciences, 51 (2), pp. 58 – 71. DOI: 10.1615/jautomatinfscien.v51.i2.70.
[12] Martsenyuk, V., Soldatkin, O., Klos-Witkowska, A., Sverstiuk, A., & Berketa, K. (2024). Operational stability study of lactate biosensors: modeling, parameter identification, and stability analysis. In Frontiers in Bioengineering and Biotechnology (Vol. 12). Frontiers Media SA. https://doi.org/10.3389/fbioe.2024.1385459.
[13] Martsenyuk V.P., Sverstiuk A.S. (2019). An exponential evaluation for recurrent neural network with discrete delays. System Research and Information Technologies, Vol. 2, 83 – 93. https://doi.org/10.20535/SRIT.2308-8893.2019.2.07
[14] Mykhaylo Palamar, Volodymyr Kruglov, Andrii Chaikovskyi Modeling Digital Radio System Secure Connection with Changing the Operating Frequency / Proceedings of the 4th IEEE International Symposium on Wireless Systems within the International Conferences on Intelligent Data Acquisition and Advanced Computing Systems (IDAACS-SWS): - 20-21 September, 2018, Lviv, Ukraine. P.:216–220. ISBN 978-1-5386-7586-1, IEEE Catalog Number: CFP18WSI-USB.
[15] Khymych, H., Dunets, V., Duda, S., Palaniza, Y., & Kornieiev, K. (2023). Dual-Polarization Yagi Antenna for Meter Wavelength Range. Radioelectronics and Communications Systems, 66(11), 609–615. https://doi.org/10.3103/s0735272722080039
[16] Nykytyuk, S. O., Sverstiuk, A. S., Klymnyuk, S. I., Pyvovarchuk, D. S., & Palaniza, Y. B. (2023). Approach to prediction and receiver operating characteristic analysis of a regression model for assessing the severity of the course Lyme borreliosis in children. Rheumatology, 61(5), 345–352. https://doi.org/10.5114/reum/173115
[17] Khvostivska L., Khvostivskyi M., Dediv I., Yatskiv V., Palaniza Y. (2023). Method, Algorithm and Computer Tool for Synphase Detection of Radio Signals in Telecommunication Networks with Noises. Proceedings of the 1st International Workshop on Computer Information Technologies in Industry 4.0. CEUR Workshop Proceedings, 173-180.